USDOT Region V Regional University Transportation Center Final Report

NEXTRANS Project No. 0103IY04

OPTIMIZED ACTIVE TRAFFIC MANAGEMENT AND SPEED

HARMONIZATION IN WORK ZONES

By
Hani Ramezani
Graduate Research Assistant
Civil and Environmental Engineering
University of Illinois, Urbana-Champaign
hrameza2@illinois.edu

and

Rahim F. Benekohal
Professor of Civil and Environmental Engineering
University of Illinois, Urbana-Champaign
rbenekoh@uiuc.edu

DISCLAIMER

Optimized Active Traffic Management and Speed Harmonization in Work Zones

Introduction

Traffic and demand management are major strategies to control delay and congestion in highway bottlenecks including work zones. The Federal Highway Administration (FHWA) introduced innovative strategies, called Active Traffic and Demand Management (ATDM) to manage congestion. Speed harmonization, known as Variable Speed Limit (VSL), is one of the ATDM strategies. In the past studies on speed harmonization, the decision variables are advisory speeds displayed by changeable message signs (CMSs); however there is another feature which is the location of the CMSs that needs to be optimally designed. Thus the objective of this study is to develop and solve a mathematical program to find the optimal location of the CMSs and displayed advisory speeds.

Findings

This study developed an optimization program and proposed a solution algorithm to find optimal advisory speeds and optimal Changeable Message Signs locations for work zones. The proposed algorithm is step-wise and the number of steps is equal to the number of signs. At each step, the location that results in minimum travel time is selected to place a sign. The algorithm was applied for a benchmark network where capacity drops for 10 minutes due to work intensity increase and traffic volume is close to the maximum capacity of the work zone. Results showed that speed harmonization can reduce delay by about 20%.

The study showed that single-regime fundamental relationships between traffic parameters may show unexpected trend in congestion conditions especially jam density might be too low, in the order of 100 pc/mi/ln. Thus multi-regime models that were developed based on work zone field

data were used in the optimization. The multi-regime models were approximated with simple functions to reduce complexity and avoid using if-then-else constraints or integer variables.

A preliminary evaluation of six solvers (CONOPT, IPOPT, Knitro, LOQO, Minos, and SNOPT) for large scale non-linear optimization was conducted and results showed that LOQO and CONOPT return feasible solutions for the benchmark problem when the solvers stops after a certain number of iterations. LOQO's final objective function value is close to CONOPT's; after 1100 iterations the final objective function value for LOQO was only 0.31% lower than that for CONOPT.

Recommendations

In the solvers evaluation all the algorithm-related options, except maximum infeasibility tolerance and the maximum number of iterations, were set to be default values. It is recommended exploring how the algorithm-related options should change to achieve desirable performance by each solver. Moreover, it is recommended a multi-objective optimization program be developed to improve both safety and traffic operation in work zones. Also, Payne model was used as a constraint to determine speed dynamics in the roadway. It is recommended this model be compared with other second order models to determine advantages and disadvantages of each for work zones.

Contacts
For more information:

Rahim F. Benekohal
Principal Investigator
Civil and Environmental Engineering
University of Illinois, Urbana Champaign -
rbenekoh@uiuc.edu

NEXTRANS Center
Purdue University - Discovery Park
2700 Kent B-100
West Lafayette, IN 47906

nextrans@purdue.edu
(765) 496-9729
(765) 807-3123 Fax

www.purdue.edu/dp/nextrans

TABLE OF CONTENTS

CHAPTER 1. INTRODUCTION

Traffic and demand management are major strategies to control delay and congestion in highway bottlenecks including work zones. The Federal Highway Administration (FHWA) introduced innovative strategies, called Active Traffic and Demand Management (ATDM) to manage congestion. According to FHWA "ATDM is the dynamic management, control, and influence of travel demand, traffic demand, and traffic flow of transportation facilities." (Federal Highway Administration, ATDM program brief: an introduction to active transportation and demand management, 2012). Examples of ATDM are speed harmonization, dynamic pricing, queue warning, etc. Although successful implementations of these strategies have been reported in the literature, there are some implementations (Lyles et al. 2004, Park and Yadlapati 2002) that resulted in insignificant improvement in traffic operation and safety, and this demands developing more efficient ATDM strategies.

Speed harmonization, known as Variable Speed Limit (VSL), is one of the ATDM strategies. There are different ideas on how speed harmonizing can improve traffic operation (Berton et al. 2002). One idea is that speed harmonization may create smooth traffic flow by reducing speed differences between vehicles and consequently it may increase capacity. Also by creating smoother flow, stop and go condition may be avoided and consequently, the likelihood of incident occurrence is reduced, and further congestion is avoided. Based on another idea, when variable speed limit affects traffic speed, it indirectly may control both arrival rate and queue propagation rate through the highway. Controlling the arrival rate could postpone the onset of flow break down and may shorten the congestion duration.

In the past studies on speed harmonization, (Kwon et al. 2007, Kamel et al. 2008, Lu et al. 2010) the decision variables are advisory speeds displayed by changeable message signs (CMSs); however there is another feature which is the location of the CMSs that needs to be optimally designed. Thus the objective of this study is to develop

and solve a mathematical program to find the optimal location of the CMSs and displayed advisory speeds.

Chapter 2 of the report reviews studies on speed harmonization for work zones and other highway bottlenecks. Chapter 3 discusses why one-regime speed-density models do not adequately describe macroscopic traffic behavior. Then it will approximate multi-regime models by simple and monotone functions to reduce computational difficulties in optimization programs. Chapter 4 formulates the optimization program to find optimal advisory speed and proposes an algorithm to determine signs locations. A benchmark problem is solved and it is discussed how to combine speed harmonization with rerouting strategy to further improve the traffic operation on the mainline. Chapter 5 evaluates some of the solvers that may be used to solve large scale optimization programs when the constraints are non-linear. Chapter 6 presents conclusions and recommendations.

CHAPTER 2. LITERATURE REVIEW ON SPEED HARMONIZATION

In this section studies on variable speed limit for work zones and other freeway bottlenecks are reviewed. Then it discusses how these studies determined the location of CMSs.

2.1   *Variable speed limit for work zones*

There are a number of VSL studies in freeway work zones. A variable speed limit control scheme was developed and tested in the field by Kwon et al. (2007). Speed and volume data were collected by radar sensors, upstream of each variable speed limit sign. The objective of the system is to reduce the average speed of vehicles at a location upstream of VSLs to the average speed of a particular point at downstream. Roughly, 30% reduction in 1-min maximum speed, 7% increase in total throughput and a 20% to 60% correlation level was reported for speed compliance.

Lin et al. (2008) developed two real-time algorithms to apply variable speed limit control. The first one tries to keep the arrival rate under a specific threshold by reducing traffic speed. Then vehicles have enough gaps to merge into the work zone. The second algorithm finds speed limits such that the queue length does not exceed a threshold. The algorithms inputs are speed and flow data from sensors. The algorithms were applied to 2-to-1, 3-to-1 and 3-to-2 work zones, simulated in CORSIM. The results showed that under "normal traffic condition" the algorithm successfully increased throughput and reduced delay.

Three control logics were presented by Park and Yadlapati (2002). Both Logic 1 and 2, reduce the difference between average speed at the vehicles in the merge area and the average speed of the arriving volume. In particular, the Logic1 computes the average speed of vehicles in the merge area during a given interval and assigns the value

to the upstream VSL sign for the next interval. On the other hand, the Logic 2 gradually reduces the speed of coming traffic using two VSL signs. The first VSL sign shows a speed limit, 10 mph higher than the average speed of the merge area while the second VSL sign displays the average speed of the merge area. The logic 3 uses a safety measure, called Minimum Safe Distance Equation (MSDE) to control the volume. The logic finds the speed of a VSL sign, changing by increment of 5 mph. If safety situation gets worse while the volume decreases or maintain at the same level, SL increases by 5 mph. All three logics were tested by simulation and it turned out that simple application of a static speed limit sign of 45 mph is better than the other logics.

McMurtry et al (2008) tested two VSL signs over a six-mile section of a work zone in Utah State. Speed data were collected to compare impacts of VSL control with the base condition. In the base condition 65-mph static speed limit was posted in the field while in the VSL control speed limit was set to 55 mph in day time and 65 mph for night time. The results showed that in day time speed variation was reduced at the beginning of the work activity area and in night time average speed was reduced.

Lyles et al. (2004) evaluated VSL on I-96, Michigan. The displayed speed limit was equal to 85th percentile speed at the next downstream location. Effects of VSL on speed distribution and travel time were assessed. It was found that VSL control had "minor effects" in the work zone.

2.2   *Variable speed limit for non-work zone bottlenecks*

VSL control has been studied for other types of freeway/highway bottlenecks. A VSL control model was develop by Breton et al (2002) for a freeway with 2 lanes per direction. The objective function was to minimize the total time spent in the network. A 15-km stretch of the freeway was divided into 1-km segments . The first 5 segments were not controlled, but the other 10 segments were equipped by VSLs. Speed and density of each segment was updated using the METANET model. Each variable speed limit was assigned to each segment. The advisory speed limit upstream of bottleneck was determined to minimize the total time spent in the network.

Allaby et al. (2007) evaluated a decision tree based algorithm for speed harmonization on freeways using microscopic simulation. The Figure 2-1 shows the original algorithm. The thresholds were selected based on engineering judgment and more adjustment may be needed to achieve better performance.

Based on the algorithm if occupancy is less than 15% speed limit is the normal speed limit. If it is more than that and volume is less than 1600 vphpl, the speed limit is the average speed of traffic. It was shown that increasing the occupancy threshold up to 20% and volume threshold up to 1800 vphpl can enhance the results.
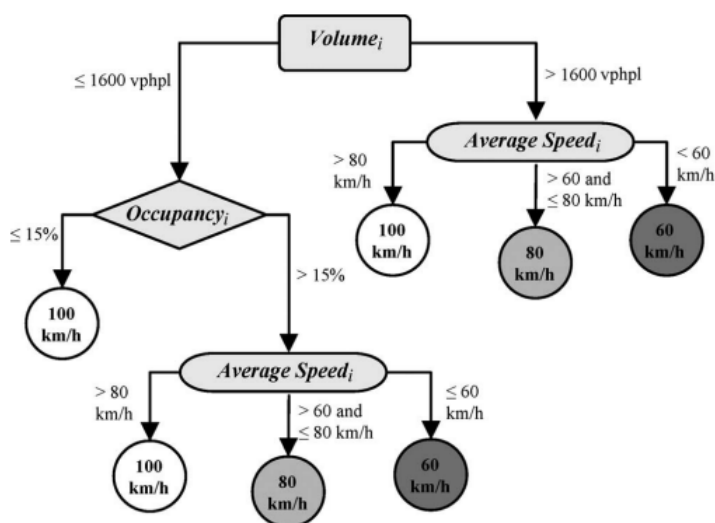
Figure 2-1: Decision tree-based algorithm for speed harmonization by Allaby et al. (2007)

Ghods et al (2007) proposed an integrated ramp metering and variable speed limit control using fuzzy logic. The if-conditions were based on speed, flow and queue occupancy rates on the main line and the then-statements were the rate of metering and the displayed speed limit. The membership functions were tuned using genetic algorithm and the algorithm was implemented to minimize the total time spent in the network. The METANET model was used to find the travel times. The model was compared with ALINEA which includes just metering algorithm the results showed the fuzzy model reduced total travel time.

In another study, Ghods and Rahimi-Kian (2008) proposed a game theory approach to design coordinated ramp metering and variable speed limit. Speed limit signs were

considered as players having the same interest. The problem was broken into subproblems, each of which was finding the speed limit for each sign as a player of the game. The results were simulated using METANET model and showed that the speed limit can be determined fast enough for real time application and better results compared with no control scenario.

Piao and McDonald (2008) evaluated safety impacts of variable speed limit on freeways using AIMSUN . The results showed that variable speed limit reduced speed difference between vehicles as well as the number of short gaps.

Kamel et al (2008) designed an integrated ramp metering and variable speed limit control to minimize number of vehicles in the on-ramp queue. The shockwave propagation and traffic speed were estimated by solving the conservation equation. The conservation equation for on and off ramps was solved using flatness method. The flatness method is an approach to solve differential equations. Using the flatness method, inputs and state variables in the differential equations can be converted to algebraic equations with no partial differential equations. How to solve the equations and the effect of the integrated system were illustrated through an example and the results showed that the integrated system is better than the "ramp metering-only' system. In particular, the maximum number of queued vehicles in the on-ramp dropped by 33%.

Lu et al (2010) minimized total time spent in the system using Variable Speed Limit system combined with ramp metering. Assuming a given ramp metering set-up speed limits were determined using Model Predictive Control. METANET model was modified for a general speed-density curve and the results of simulation in MATLAB showed that the system enhance traffic operation.

Wang (2011) developed a macroscopic model to use in traffic control problems. The model is a combination of the second order density-speed model and a car following model. When vehicle speed is less than the speed limit, traffic speed is derived from the second order model and when it is above the speed limit drivers slowdown in response to the speed limit and their speed in the next time step is estimated using the car following model based on the difference between the current speed and the speed limit. The model was tested in VISSIM for a 5-lane unidirectional freeway when traffic is in free flow

condition as well as congested conditions due to accident. The results showed that the performance of the model matched VISSIM.

Su et al (2011) proposed a combined ramp metering and VSL control scheme for weaving sections. The VSL control strategy keeps the occupancy at the critical level for the discharge section by displaying the critical speed as speed limit. On the other hand speed limit gradually decreases when vehicles reach the back of queue. The ramp metering control strategy minimizes delay and maximizes travel time. The simulation showed that the system improves the system performance when deriver compliance is beyond 30%.

Lu et al (2011) developed a combined ramp metering and VSL control strategy. First the ramp metering rate was determined by minimizing travel time and maximizing mainline flow. Then VSL strategy was designed such that it creates a discharge point before the bottleneck. Within queue speed limit was equal to the critical speed and free flow speed gradually decreased to the critical speed at the back of queue.

Kwon et al (2012) designed a VSL strategy to avoid sudden deceleration. The beginning of the control zone was determined when speed is less than 55 mph for the current interval and deceleration rate is less than or equal to 1500 mile/hr, for three consecutive intervals. These thresholds were determined by observing 20 incidents during a 3-month period and it turned out that half of them happened when downstream speed is less than 55 mph and deceleration rate is less than or equal to 1500 mile/hr. The displayed speed limit was determined based on the distance between the signs and deceleration rate of the traffic. The system status was updated every 30 sec. Simulation results showed that the system reduces sudden deceleration with relatively small increase in travel time.

Hadiuzzaman and Oiu (2012) incorporate capacity drop in cell transmission model to design a VSL strategy for a lane drop. Model Predictive Control was used to determine the speed limits and the modified cell transmission model was evaluated in VISSIM and it showed about 7% increase in the flow rate for the modeled freeway section.

2.3 *Discussion*

Distance between the signs was not incorporated as a decision variable in past studies; However in some studies, the location of the signs was determined based on comfortable and safe deceleration rate, or based on characteristics of bottlenecks.

To provide comfortable deceleration, Kwon et al. (2012) and Lin et al. (2004) recommended that spacing between two consecutive speed limit signs (d_i) should be at least equal to

$$d_i = \frac{SL_i^2 - SL_{i+1}^2}{2a}$$

2-1

Where SL_i and SL_{i+1} are speed limits displayed by two consecutive signs and a is the average deceleration rate.

There are some studies that determined the signs location based on the network characteristics. Allaby et al. (2007) assumed that speed limit signs are installed next to loop detectors and this resulted in 13 signs with spacing of 500-600 metre for an 8-km section of a highway. In another study, Su et al. (2011) optimized Variable Speed Limit (VSL) combined with ramp metering, and they assumed that VSL signs will be used where on-ramps merge the mainline. Thus 7 signs were used for a 10-km stretch of a highway. Park and Yadlapati (2002) applied two VSL sings on a 2.5 mile work zone. The first one is posted where the first "Road WORK AHEAD" sign is located (2950 ft upstream of transition taper). The second one is placed close to "LANE ENDS MERGE LEFT" sign (980 ft upstream of bottleneck).

There are also studies that did not provide any discussion for the sign placement, but some values were chosen for spacing between the signs in the example problems solved. For instance, Berton et al. (2004) used 10 signs with spacing of 1 km and Ghods et al. (2007) used 3 signs with 1 km spacing.

The distances used in the reviewed studies ranges from 0.3 miles (500 m) to roughly a mile. These values are not determined from an optimization program and may not cause an optimal operation. For instance, the values around 0.3 miles may be considered to be short and some of the signs may be redundant causing extra cost. Also in most of the

studies, the distances between the signs are equal; however for optimal operation, the distances may change as traffic moves toward the bottleneck. For instance, the distance between the signs that are closer to the bottleneck might be shorter to provide more control on traffic. Thus this study determines the distance between the signs through an optimization program and provides implementation knowledge by solving the problem for different traffic conditions.

CHAPTER 3. FUNDAMENTAL RELATIONSHIPS BETWEEN THE TRAFFIC
PARAMETERS

Speed harmonization relies on fundamental relationships between the traffic parameters (e.g. speed-density relationships) to predict traffic state and determine proper advisory speeds. One-regime speed-density relationships have been used in several speed harmonization studies (Berton et al. 2004, Ghods et al. 2007). Using one-regime models would reduce problem complexity and help solving optimization program; however they may not adequately describe the relationship between traffic parameters. Example of those one-regime models is exponential equation, defined as below.

$$V(D) = V_f \exp\left(\frac{-1}{a}\left(\frac{D}{D_{cr}}\right)^a\right)$$
<div align="right">3-1</div>

Where

D: Road density (pc/mi/ln),

V(D): Speed (mph) corresponding to density D,

V_f: Free flow speed (mph),

D_{cr}: Critical density (i.e. density at capacity), and

a: Parameter of the equation.

The parameter "a" can be determined such that the maximum flow rate from the equation returns the roadway capacity; however it is shown that an exponential equation that matches free flow speed, critical density and capacity of a roadway may not properly reflect density-speed relationship in oversaturated conditions. For instance, if the HCM 2010 relationship for basic freeway sections with free flow speed of 65 mph is approximated by the exponential equation, the parameters will be V_f=65, D_{cr}=45, and a=4.569. These

parameters return the same free flow speed, capacity and critical density as the HCM 2010 relationship does for free flow speed of 65 mph. Figures 3-1a and b depict the HCM 2010 curves versus approximated curves by the exponential equation.
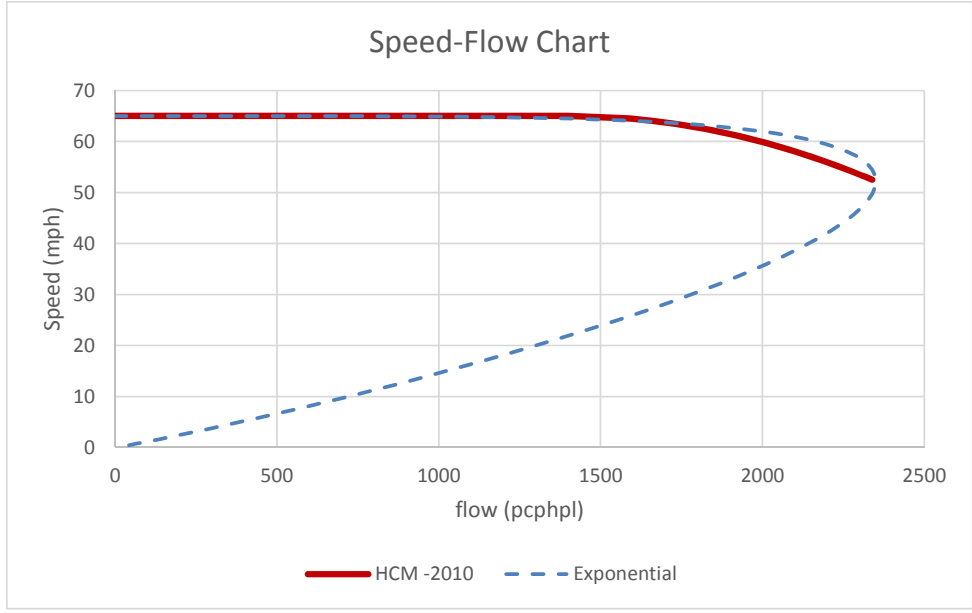
Figure 3-1 a
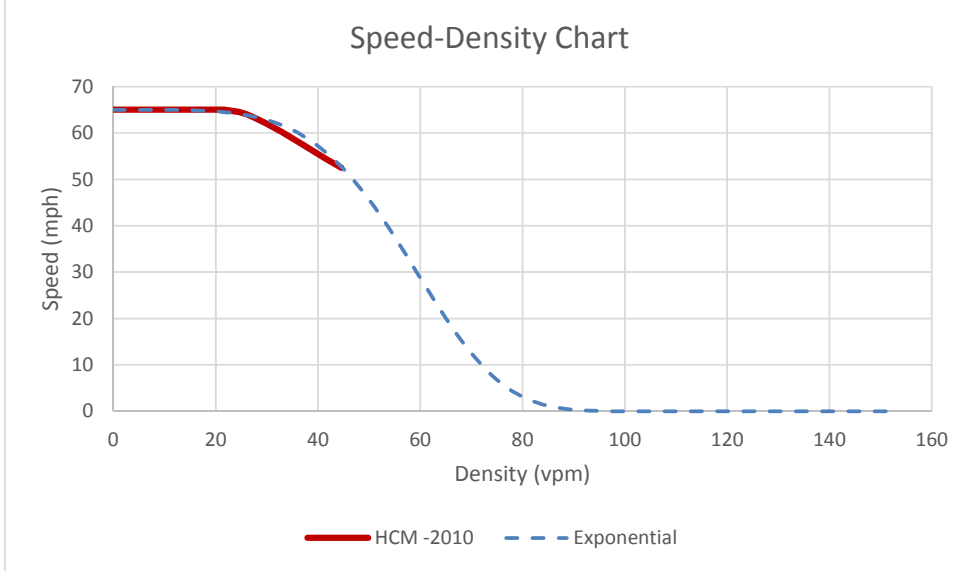
Figure 3-1 b

Figure 3-1: The HCM-2010 relationship approximated by the exponential equation a)speed-flow chart b) speed-density chart

The HCM-2010 relationship is just developed for undersaturated conditions ($52.22\leq$ speed$\leq$65) . Within this domain, the approximated speed-flow curve matches beginning and end of the HCM curve with some discrepancies in speed when volume is close to capacity (See Figure 3-1a). If one limits himself to the speed-flow curve, exponential equation may reflect acceptable behavior; however speed-density curve reveals that the behavior of the exponential curve for oversaturated conditions is not intuitively expected. In particular, based on the speed-density curve, the jam density (assume density when speed is 1 mph) is about 90 pc/mi/ln which is translated to average spacing of 58 ft when traffic is composed of just passenger cars and they are stopped. This spacing is considerably higher than expected spacing values (around 20 ft when average car length is 15 ft) in stopped queues. This might be an indication that rate of speed drop in speed-density relationship is too high for oversaturated conditions. Thus the approximated curve is not sufficient to describe the oversaturated conditions, and this is the motivation to incorporate multi-regime models in the optimization program for speed harmonization.

Incorporating multi-regime models, as the way they are, may cause numerical difficulties in large scale optimization programs. One of the reasons is that the form of equations might be polynomial or in a more complex form that requires the program to compute and evaluate gradient and Hessian matrices causing more numerical difficulties. Moreover, although multi-regime models might be suitably developed to describe relationships between two parameters, for instance speed versus flow, it may not be easy to transform them to relationships between other traffic parameters (e.g. speed versus density). Thus this section tries to approximate each regime with linear or another monotone function to reduce numerical difficulties and to provide the flexibility of transforming the equations.

In this study, approximated versions of HCM 2010 speed-flow relationship for basic freeway sections and four-regime speed-flow relationship developed by Benekohal et al. (2010) for work zones are used to avoid the numerical difficulties.

3.1 *Approximation for HCM 2010 speed-flow relationships*

The approximation method is explained in details for the HCM 2010 relationship when free flow speed is 75 mph in basic freeway sections. Similar approach is applied for other free flow speeds and the final results will be reported for them in this section.

There are two regimes in HCM-2010 relationships for basic freeway sections:

$$V = \begin{cases} FFS & F < F_B \\ FFS - a(F - F_B)^2 & F \geq F_B \end{cases} \qquad 3\text{-}2$$

Where

F : Flow rate (pcphpl),

V: Speed (mph),

 FFS: Free flow speed and equals to 75 mph,

a : Model coefficient and is equal to -0.00001107, and

F_B: Flow rate at the breakpoint which is equal to 1000 pcphpl.

The approximation includes two steps. In step 1, only the transition regime (polynomial equation) is approximated by a line as shown in Figure 3-2. The maximum speed discrepancy between the approximated curve and the HCM curve is about 5.4 mph with average error of -3.6 mph.
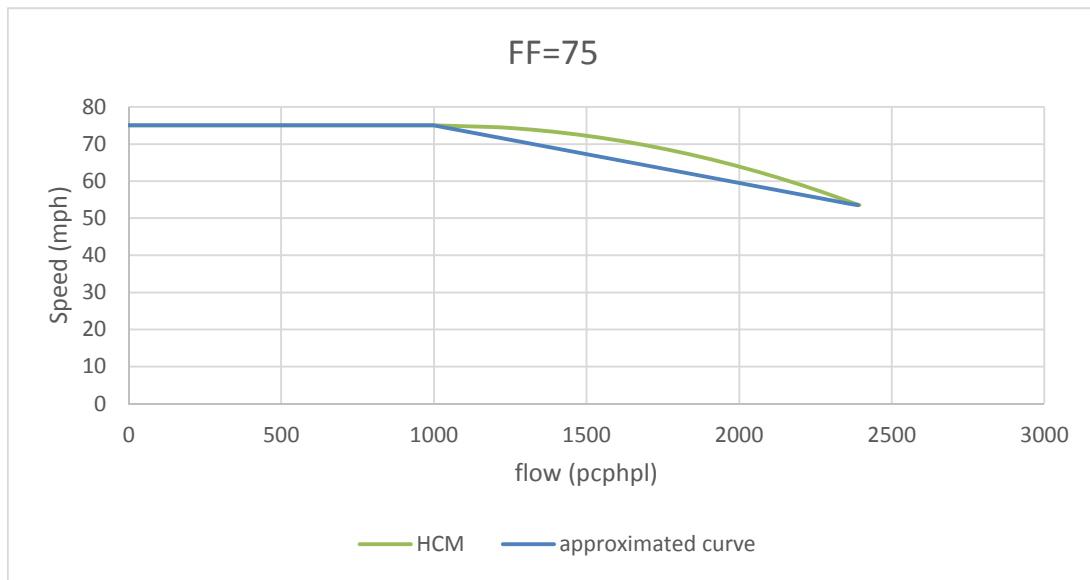
Figure 3-2: Step 1 in HCM 2010 speed-flow curve approximation

Step 2 reduces the discrepancies by increasing the break point for the approximated curve. The formula for the approximated curve is:

$$V = \begin{cases} FFS & F < F_B{}' \\ FFS + \dfrac{V_C - FFS}{F_C - F_B{}'}(F - F_B{}') & F \geq F_B{}' \end{cases} \qquad 3\text{-}3$$

When $F_B{}' = F_B = 1000$ the approximated curve is the same as that shown in Figure 3-1a. Table 3-1 reports the maximum absolute error and average error for different values of $F_B{}'$ with increment of 100. The break point of 1400 will result in the lowest maximum absolute error with the average error of -0.50 mph which in magnitude is close to minimum of 0.27 at break point of 1500. Hence $F_B{}'$ is chosen to be 1400 pcphpl when free flow speed os 75 mph.

Similar approach is applied for the other free flow speeds and Table 3-2 reports $F_B{}'$ that has been selected for different free flow speeds. One can use Equation 3-3 with the parameters defined in Table 3-2 to approximate HCM 2010 relationships for basic freeway sections.

Table 3-1: Error in speed estimation for different break points

FFS	Maximum absolute error (mph)	average error (mph)
1000	5.41	-3.59
1100	4.61	-2.82
1200	3.75	-2.05
1300	2.85	-1.27
1400	1.94	-0.50
1500	2.77	0.27
1600	3.99	1.04

Table 3-2: Parameters for the approximated speed-flow curves

FFS	F_C (capacity)	V_C (speed at capacity)	F_B (break point)
75	2400	53.3	1400
70	2400	53.3	1500
65	2350	52.2	1600
60	2300	51.1	1700
55	2250	50	1800

Still the HCM-2010 relationships do not have any equations for the oversaturated conditions. Benekohal et al (2010) showed power functions can adequately describe congestion data from work zones. The general form of the power function is

$$F = aV^b \qquad\qquad 3\text{-}4$$

Where a and b are the coefficients of the equation. The same form of equation is used for basic freeway sections with new coefficients which are different from those for work zones. The coefficients a and b are found such the power function connects capacity point to the point with jam density. It is assumed that jam density is 250 pc/mi/ln and occurs at speed of 1 mph. This jam density is corresponding to average spacing of 21 ft when all vehicles are passenger cars. Capacity and corresponding speed also can be obtained from Table 3-2. The resulting coefficients are displayed in Table 3-3 for different free flow speeds.

Table 3-3: Coefficients of the congestion part of the approximated speed-flow curves for basic freeway sections

FFS	A	b
75	250	0.5688
70	250	0.5688
65	250	0.5665
60	250	0.5641
55	250	0.5617

Figure 3-3 shows the approximated curves for free flow speed of 75 mph.
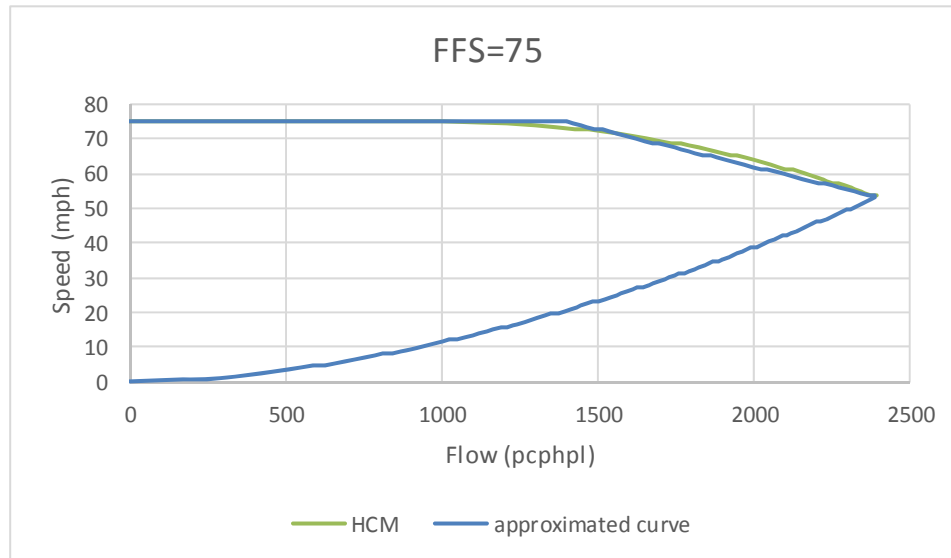
Figure 3-3 b
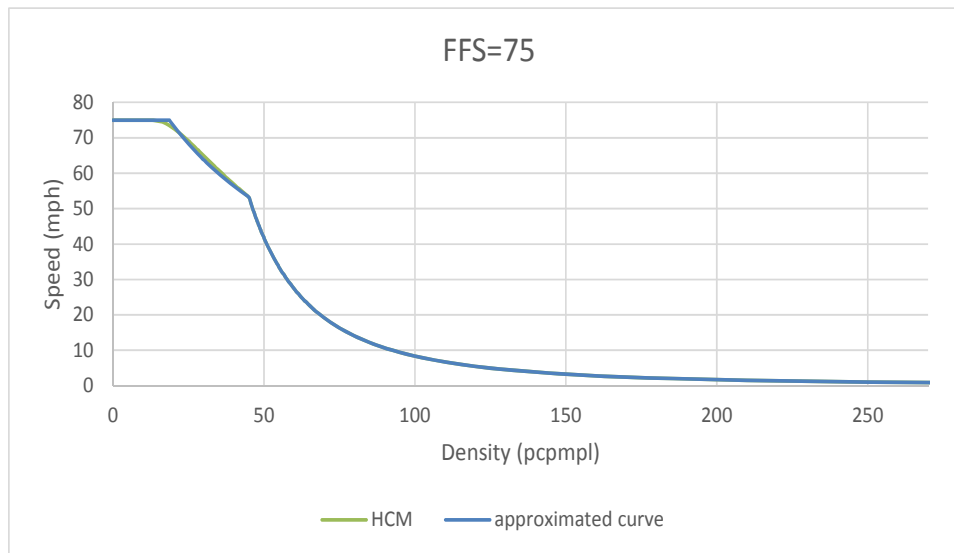
Figure 3-3 a

Figure 3-3: HCM 2010 curves for FFS=75 mph versus approximated curves a) speed-flow curves
b) speed-density curves

3.2   Approximation for work zone speed-flow relationships.

Benekohal et al (2010) developed four-regime speed-flow relationships for work zones as shown in Figure 3-4. The four regimes are: 1) free flow, 2) upper transition, 3) lower transition, and 4) congestion. The two transition regimes are four-degree polynomial splines that potentially may create computational difficulties to compute gradient and Hessian matrices. Moreover, there is not always a closed form equation which strictly defines speed versus density or speed versus flow for these regimes. Thus the curves are approximated with simpler functions. How to approximate the curves are explained for speed limit of 45 mph and 55 mph.
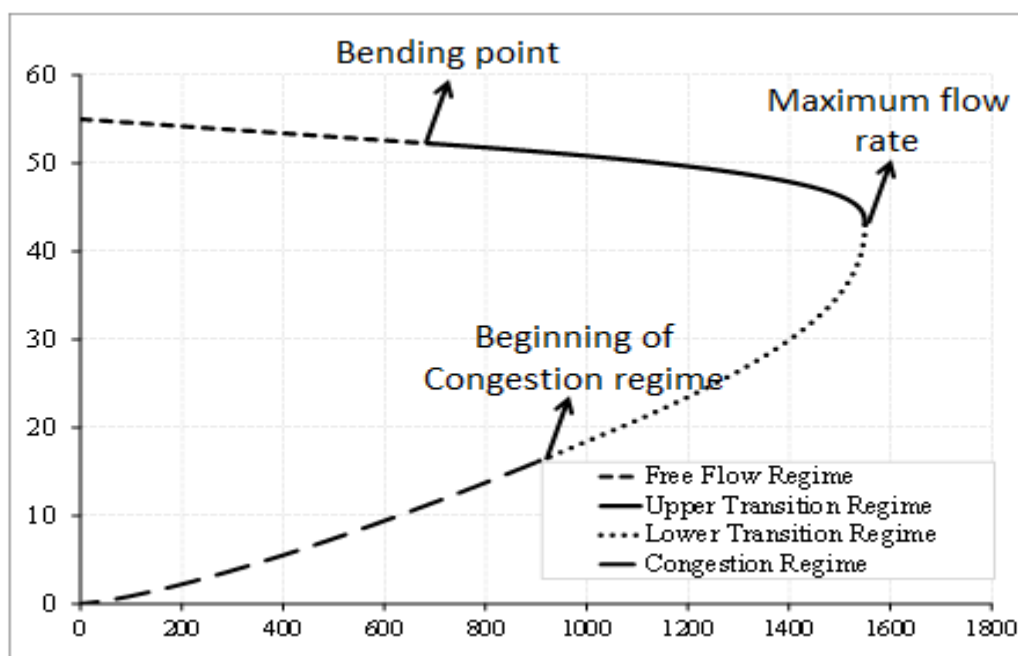
Figure 3-4: General form of four-regime speed-flow relationships

Similar to HCM-2010 curves, the following relationships are used to approximated the undersaturated part of the work zone speed-flow relationships:

$$\begin{cases} K & 0 \leq F < F_B \\ K + \dfrac{V_C - K}{F_C - F_B}(F - F_B) & F_B \leq F < F_C \end{cases} \qquad 3\text{-}5$$

K for the curves with speed limit of 55 mph is equal to the intercept in the original curve while for the curves with speed limit of 45 mph it is equal to the speed at the break point. The break point is connected to the capacity point using a line.

The choice of K for speed limit of 45 mph creates some discrepancies when traffic volume is low because the free flow regime is an inclined line. However the discrepancy reduces at higher volumes (zero at break point) which is more important for congestion management.

For oversaturated part, a power function (See Equation 3-4) connects the point with jam density to the capacity point. Similar to approximations for HCM-2010 curves, a jam density of 250 with speed of 1 mph is used for the work zone curves. Table 3-4 shows the coefficients of the approximated speed-flow curves for work zones and Figures 3-5 and 3-6 demonstrates four regimes curves and approximated curves for speed limit of 55 mph and 45 mph. respectively.

Table 3-4: Coefficients of the approximated speed-flow curves for work zone

SL	Coefficients for undersaturated part				Coefficients for oversaturated part	
	K	F_B	F_C	V_C	a	b
55	55.00	729	1614	47.0	250	0.4871
45	42.74	566	1350	37.7	250	0.4681
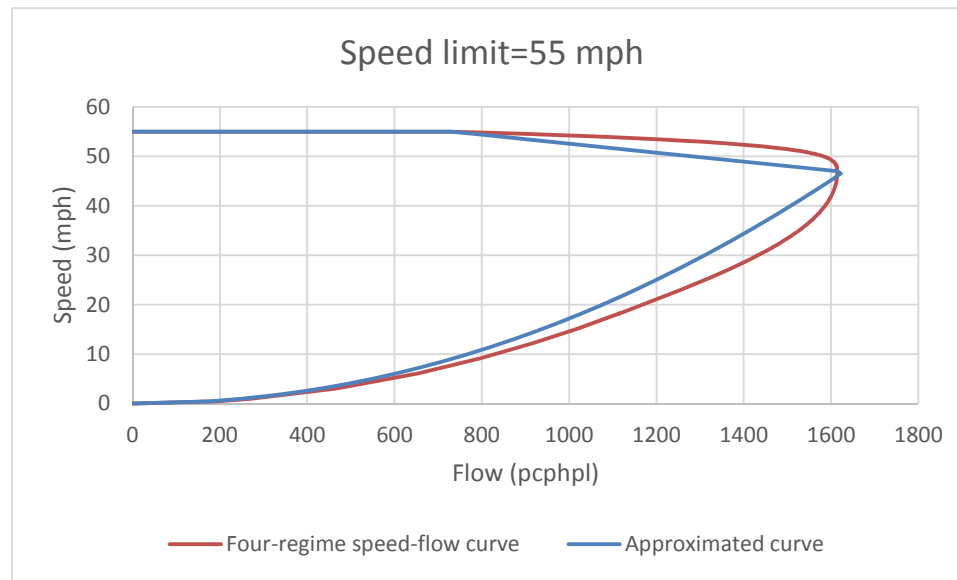
Figure 3-5 a
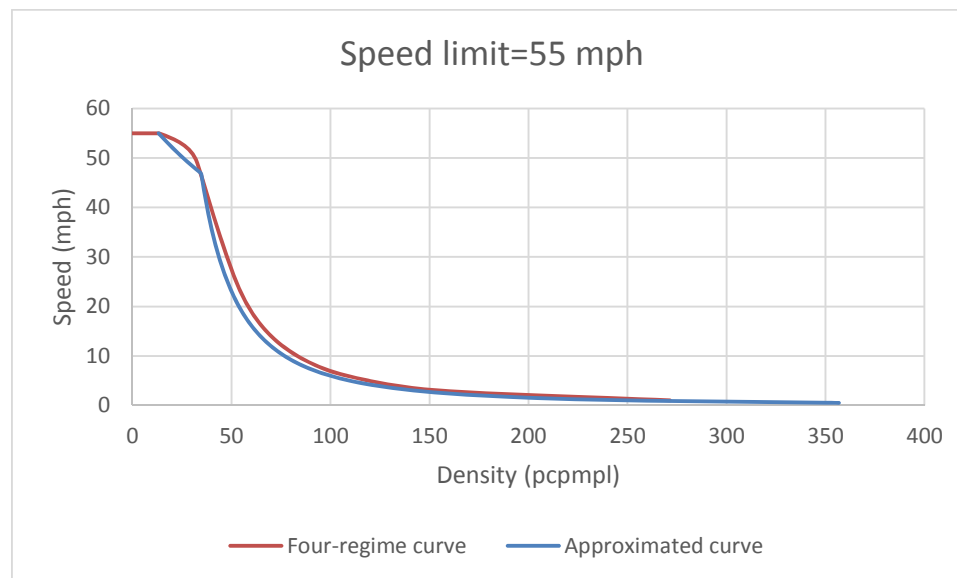
Figure 3-5 b

Figure 3-5: Four-regime curves for work zones with speed limit of 55 mph a) Speed-flow curve b) speed-density curve
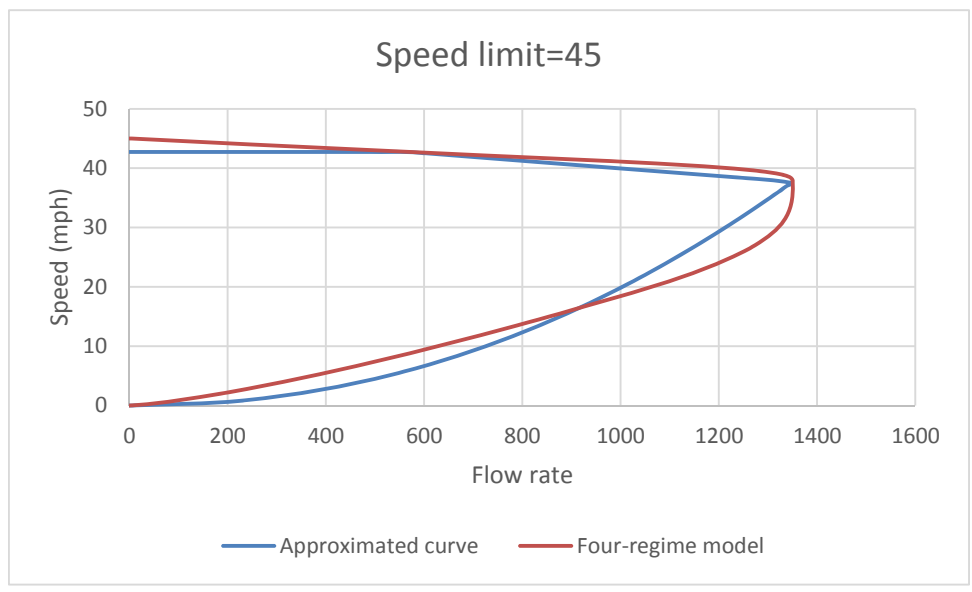
Figure 3-6 a
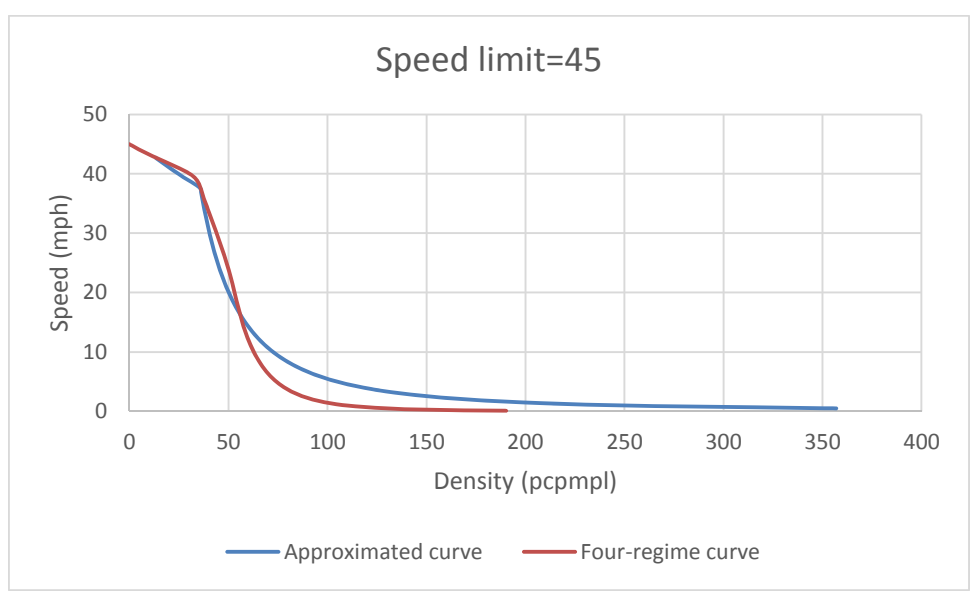
Figure 3-6 b

Figure 3-6: Four-regime curves for work zones with speed limit of 45 mph a) Speed-flow curve b) speed-density curve

3.3 *Formulation of the multi-regime models in optimization programs*

Usually, speed-density relationships are used to determine traffic state in optimization programs for speed harmonization. Now, the speed-density relationships can be easily derived from the approximated speed-flow relationships discussed in the previous sections. The approximated speed-flow models are composed of three equations: two linear equations for the undersaturated part and one power function for the oversaturated part. Similarly speed-density models are composed of three equations and assume they are expressed as

$$V(D) = \begin{cases} R_1(D) & D < D_B \\ R_2(D) & D_B \leq D < D_C \\ R_3(D) & D_C \leq D \end{cases} \qquad \text{3-6}$$

Where D_B and D_C are the densities at break point and capacity, respectively. $R_1(D)$ and $R_2(D)$ are the functions that are used to compute speed in undersaturated condition and $R_3(D)$ is used in oversaturated condition.

Incorporating the above multi-regime model in optimization program requires modeling logical constraints (if-then-else constraints). Usually integer variables are used to model logical constraints and this makes the problem more complex; however sometimes we can prevent integer variables when the constraints have specific properties. For the approximated multi-regime models, one can verify that the following relationship holds

$$V(D) = min\{\, R_1(D), R_2(D), R_3(D)\} \qquad \text{3-7}$$

One can make pair-wise comparisons and use the following expressions to avoid defining integer variables.

$$V'(D) = min\{\, R_1(D), R_2(D)\} \qquad \text{3-8}$$

$$= \frac{R_1(D) + R_2(D)}{2} - \left| \frac{R_1(D) - R_2(D)}{2} \right|$$

$$V(D) = min\{ V'(D), R_3(D)\} \qquad \text{3-9}$$

$$= \frac{V'(D) + R_3}{2} - \left| \frac{V'(D) - R_3(D)}{2} \right|$$

CHAPTER 4. PROBLEM FORMULATION AND SOLUTION

The formulation is presented for typical 2-to-1 highway work zones (i.e. one of the two lanes is open in a given direction) The following assumptions are made:

- It is assumed that the initial condition is known meaning that traffic states through the work zone are given, and they are in undersaturated conditions.
- Base speed-flow curves for the sections are available.
- The roadway and time are discretized, and suppose that L and Δt denote the section length and the time interval length, respectively. The discretized network is shown in Figure 4-1. Traffic moves from right to left, and it is assumed that lane drop occures abruptly at the beginning of the transition area.
- It is assumed that vehicles fully comply with the displayed advisory speeds.

It is intended to determine

1) Location of CMSs
2) Displayed advisory speed by each CMS during each time interval.

First the optimization program is formulated to find optimal advisory speeds assuming the location of the signs are known then an algorithm is presented to determine the sings locations.
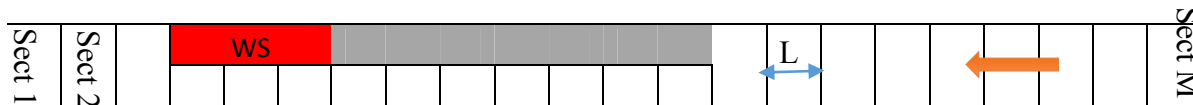
Figure 4-1: Discretized Network

4.1   *Definitions*

The definitions of the decision variables are:

$AS_{i,t}$: Advisory speed that is in effect in the section i during the time interval t. If there is a CMS at the upstream boundary of the section i then $AS_{i,t}$ is the speed displayed by the CMS. If there is no CMS at the upstream boundary of the section i, then $AS_{i,t}$ is the displayed speed by the closest CMS that is located at the upstream of the section i. Other than this decision variable, there are the following variables in the program determining the state of the system:

$V_{i,t}$: Average travel speed (mph) for the section i at the beginning of interval t

$D_{i,t}$: Density (vpmpl) for the section i at the beginning of interval t

$F_{i,t}$: Flow rate (vphpl) exiting from the section i at the beginning of interval t

$V(D_{i,t})$: Speed corresponding to density $D_{i,t}$ computed from speed-density relationship for the section i and time interval t.

λ_i: The number of open lanes for the section i.

$U_{i,t}$: Steady state speed for the section i and time interval t. it is the minimum of $V(D_{i,t})$ and $AS_{i,t}$.

M: Total number of sections

N_t: Number of time intervals in the study period

Δt: Time interval length for updating the state of traffic

τ, ϑ: Speed dynamics parameters

TTT: Total travel time (veh-hr)

I:set of all section indices

I^*:set of section indices with a CMS at the upstream boundary of the sections

T: set of all time interval indices

4.2   Objective function formulation

The objective function is to minimize the total travel time for sections that represent the bottleneck and the sections that are located upstream of the bottleneck and can be driven as below

$$TTT = \sum_i \sum_t Avg\ travel\ time * exit\ flow * no.of\ open\ lanes\ * interval\ length$$

$$= \sum_i \sum_t \frac{L}{V_{i,t}} * F_{i,t} * \lambda_i * \Delta t$$

This function is nonlinear with respect to $F_{i,t}$ and $V_{i,t}$. One can replace $\frac{F_{i,t}}{V_{i,t}}$ by $D_{i,t}$ and remove the constants L and Δt to achieve the following objective function which is linear with respect to $D_{i,t}$ and easier to evaluate by solvers.

$$\frac{TTT}{L * \Delta t} = \sum_i \sum_t D_{i,t} * \lambda_i \qquad\qquad 4\text{-}1$$

4.3   Constraints formulation

The constraints can be divided into two sets:

     1) Traffic evolution constraints

     2) Safety constraints

Each set is formulated as below.

4.3.1   **Traffic evolution constraints**

The purpose of these constraints is to find average travel speed, exit flow, average density for a given section at the beginning of the time interval t+1, assuming that all these variables are known at the beginning of interval t.

Constraint 1) Traffic density is estimated using the conservation law:

$$D_{i,t+1} * L = D_{i,t} * L + \left(F_{i+1,t} * \lambda_{i+1} - F_{i,t} * \lambda_i\right) * \Delta t \qquad \forall i \in I, \forall t \in T \qquad 4\text{-}2$$

Constraint 2) Compute speed using the Payne model

$$V_{i,t+1} = V_{i,t} + \frac{\Delta t}{L} V_{i,t} (V_{i+1,t} - V_{i,t}) + \frac{\Delta t}{\tau} (U_{i,t} - V_{i,t}) - \frac{\Delta t * \vartheta}{\tau * L} \left(\frac{D_{i-1,t} - D_{i,t}}{D_{i,t}} \right) \qquad \forall i \in I, \forall t \in T \qquad \text{4-3}$$

Constraints 3) The Constraints 3 to 5 find the minimum of the advisory speed and the speed from the speed-density relationship and assign it to the steady state speed, $U_{i,t}$, in Constraint 2 .

$$U_{i,t+1} \leq V(D_{i,t}) \qquad\qquad \forall i \in I, \forall t \in T \qquad \text{4-4}$$

How to formulate multi-regime speed-density relationships is discussed in Section 3.3.

Constraints 4)

$$U_{i,t+1} \leq AS_{i,t+1} \qquad\qquad \forall i \in I, \forall t \in T \qquad \text{4-5}$$

Constraints 5)

$$(U_{i,t+1} - V(D_{i,t}))(U_{i,t+1} - AS_{i,t+1}) = 0 \qquad\qquad \forall i \in I, \forall t \in T \qquad \text{4-6}$$

Constraints 6) The Constraint 6 finds exit flow rate

$$F_{i,t+1} = D_{i,t+1} * V_{i,t+1} \qquad\qquad \forall i \in I, \forall t \in T \qquad \text{4-7}$$

4.3.2 Safety constraints

Constraints 7) The constraint is developed to restrict advisory speed changes by 5 mph.

$$AS_{i+1,t} - AS_{i,t} \leq 5 \qquad\qquad \forall i \in I^*, \forall t \in T \qquad \text{4-8}$$

Constraint 8)

When there is CMS at the boundary of two consecutive sections, the effective advisory speeds are equal

$$AS_{i+1,t} - AS_{i,t} = 0 \qquad\qquad \forall i \in I - I^*, \forall t \in T \qquad \text{4-9}$$

Constraints 9) The Constraint 7 is to control spatial advisory speed changes while the Constraint 9 is to control advisory speed fluctuations for a given sign over time.

$$|AS_{i,t+1} - AS_{i,t}| \leq 5 \qquad\qquad \forall i \in I^*, \forall t \in T \qquad 4\text{-}10$$

Constraints 10) The advisory speeds should not exceed the static speed limits established based on the work zone design standards. Thus a maximum speed limit ($MaxSL_i$) is considered for each section in this constraint. Depending on the work intensity and how restricted the work zone condition is, these speed limits might be 65 mph, 55 mph, or 45 mph. Usually in the beginning of typical 2-to-1 work zones where there are two lanes open, the speed limit is 65 mph. As traffic moves toward the lane closure the speed limit drops to 55 mph and if work intensity is high, the speed limit further reduces to 45 mph in vicinity of the work space. After passing the work space, the speed limit usually comes back to 65 mph, which is the speed limit for the normal section of the roadway.

$$AS_{i,t} \leq MaxSL_i \qquad\qquad \forall i \in I^*, \forall t \in T \qquad 4\text{-}11$$

Constraints 11) this constraint establishes the minimum advisory speed to be MinAS. In this study MinAS of 35 mph is used.

$$MinAS \leq AS_{i,t} \qquad\qquad \forall i \in I^*, \forall t \in T \qquad 4\text{-}12$$

4.4   Algorithm to determine signs locations

An iterative algorithm is proposed to determine the locations of N signs within the control zone. The control zone is the set of the sections where CMSs can be potentially located. The algorithm finds the location of the signs consecutively.

For the first sign, the algorithm looks for the location that results in the minimum travel time. In particular, one sign is located in a given section and the optimization program that is formulated in Sections 4.2 and 4.3 is solved. Similarly the sign is placed in other sections and corresponding objective function values are obtained. The section that

results in minimum objective function value is selected as the permanent location for the first sign.

Then given the location of the first sign, the location of the second sign is found by putting the sign on possible locations and evaluating the corresponding objective function values. A minimum number of sections (or distance) between two consecutive signs is considered as a hard constraint. In other words, the number of sections between two consecutive CMSs has to be greater than Minsec which is computed as below:

$$\text{Minsec} = \left\lceil \frac{\text{Total number of the sections in } I_c}{2 * N} \right\rceil \qquad 4\text{-}13$$

If the distance between two signs is less than or equal to Minsec, then they are considered in the neighborhood of each other. Applying the above-mentioned constraint, the location of the second sign that result in the best objective function is determined. Similarly the location of the remaining signs are found. The algorithm is presented as below:

Define:

I_c: the set of section indices in the control zone

I^*: set of section indices with a CMS at the upstream boundary of the sections

I_p^*: set of section indices that permanently have been selected

Step 0: $I_p^* = \emptyset$, n=0

Step 1: Determine all section qs that have the following three criteria:

1) It is in the control section $(q \in I)$
2) It has not been permanently selected $(q \notin I_p^*)$
3) It is not in the neighborhood of any sections in I_p^* $(|q\text{-}p| > \text{Minsec } \forall p \in I_p^*)$

Then for each section q:

$$I^* := I_p^* \cup \{q\}$$

Solve the optimization program to determine the optimal advisory speeds

Step 2: Determine q_{min} which resulted in the minimum objective function in step 1 and update I_p^*

$$I_p^* := I_p^* \cup \{q_{min}\} \text{ and } n=n+1$$

Step 3: If n=N then stop otherwise go to step 1

4.5   Benchmark problem

It is intended to determine the location of four signs for the roadway shown in Figure 4-2. traffic moves from right to left and the roadway includes three parts:

1) 2-lane sections upstream of the work zone. The length of the 2-lane section is 13 miles. It is assumed that free flow speed for these sections is 65 mph and the corresponding speed-flow relationship that is proposed by HCM 2010 for basic freeway sections is used.

2) 1-lane section: The length of this part is 7 miles and it is assumed that speed limit and free flow speed are 45 mph. As shown in Figure 4-2, three miles of this part represents work space and no work activity occurs within the rest of this part.

3) The two lane sections after the work zone: the length of this part is 3 miles. This sections were considered to avoid effects of boundary conditions on the traffic state computations for work space.
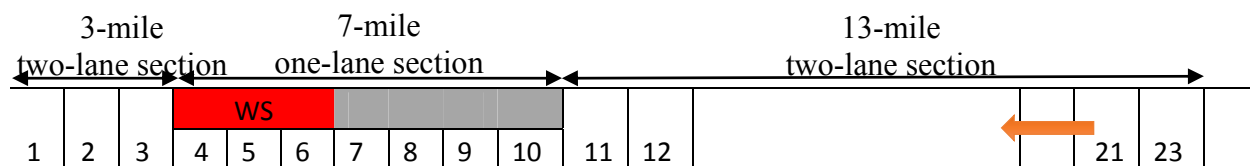
Figure 4-2: Benchmark problem network

The roadway is discretized with 1- mile long sections. Thus the whole network includes 23 sections. The length of time intervals is 15 seconds. The traffic volume in the 2-lane section is 650 pcphpl (i.e. 1300 pcphpl in the 1-lane section). Capacity of the work space is 1315 pcphpl and it is 2350 pcphpl for the 2-lane section. However capacity in

the work space drops to 800 pcphpl for 10 minutes and creates queue. Back of queue reaches 4 miles upstream of work space and congestion completely dissipates roughly 1.25 hr after the time that capacity reaches to the 1315 pcphpl.

4.5.1 Parameter set up

Optimization program is run for 350 intervals (roughly 1.50 hr). This duration was selected based traffic conditions when there is no speed harmonization. After roughly 350 intervals congestion completely dissipates and traffic conditions come back to that before capacity drop. In particular the difference between the sections densities in the beginning and end of analysis period is less than 2 vehicle. The capacity drops occurred at the beginning of interval 11 and lasts until the end of interval 50 (for 10 minutes)

The Payne's model parameters, τ and ϑ, are selected to be 18 seconds and $65\frac{km^2}{h}$ (=25 $\frac{mile^2}{h}$) respectively as used by Kotsialos et al. 1999 and Berton et al. 2004. The control sections are the sections at upstream of the work space (i.e. Sections 7 to 23). It is assumed that density at the exit section, Section 1, and its downstream section is equal as there is no queue after the work space.

4.5.2 Determining the signs locations

The solver that is used for the benchmark problem is LOQO. Chapter 5 evaluates the performance of some of the solvers that are available for large scale optimization. Based on the results of the evaluation LOQO was found more suitable for the benchmark problem. The algorithm to determine signs location was implemented for the benchmark problem. The control section includes 17 sections (from section 7 to section 23) and the number of signs is 4; thus based on Equation 4-3, Minsec is computed to be 2.

Figure 4-3 shows how objective function changes for different CMSs. The minimum objective function value for the first sign is achieved when the first sign is placed in Section 23 (i.e. at the upstream boundary of the Section 23). As the first CMS moves closer to work space the objective function increases until section 10 that the objective function is almost equal to the corresponding value in the Base condition (i.e. when there is no sign).

The Minsec is 2 and the Section 23 has been already chosen for the first sign hence the Sections 22 and 21 are not explored for the second sign. All possible locations for the second sign which is coupled with the CMS in the Section 23 are explored and Section 20 is chosen for the second signs as it has the minimum objective function value. Overall, as the second sign moves toward the work space the objective function increases. However, this trend is not true for the third and fourth signs. Based on the evaluations of the objective function, the third and fourth CMSs should be placed at Sections 17 and 13, respectively.
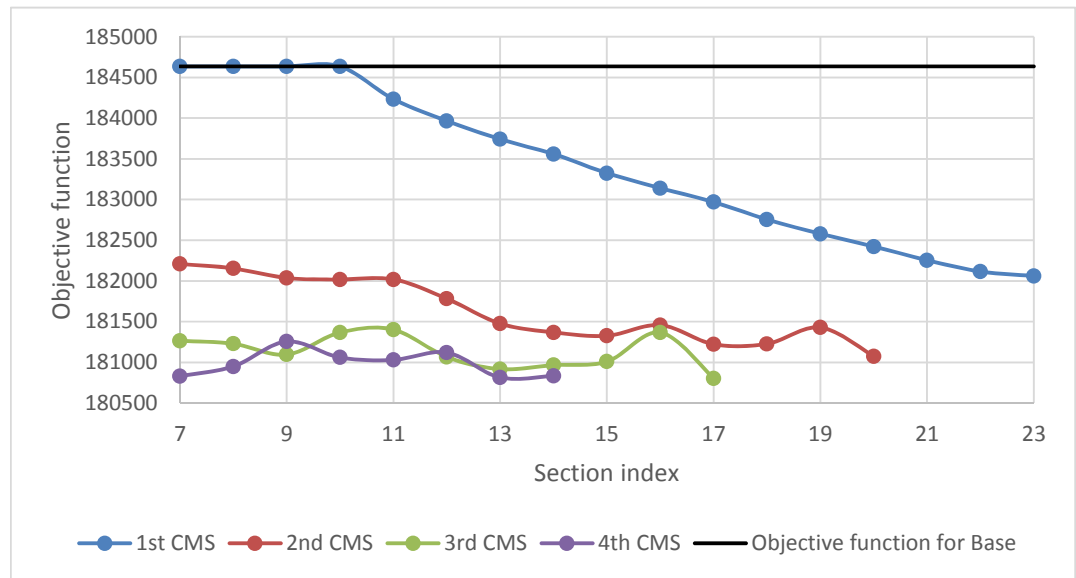
Figure 4-3: Determining signs locations

4.5.3 Determining advisory speeds

The displayed advisory speeds by the CMSs are shown in Figure 4-4. The CMSs display the minimum speed when there is work activity (between intervals 10 and 51) trying to reduce arrival rate to control congestion propagation.
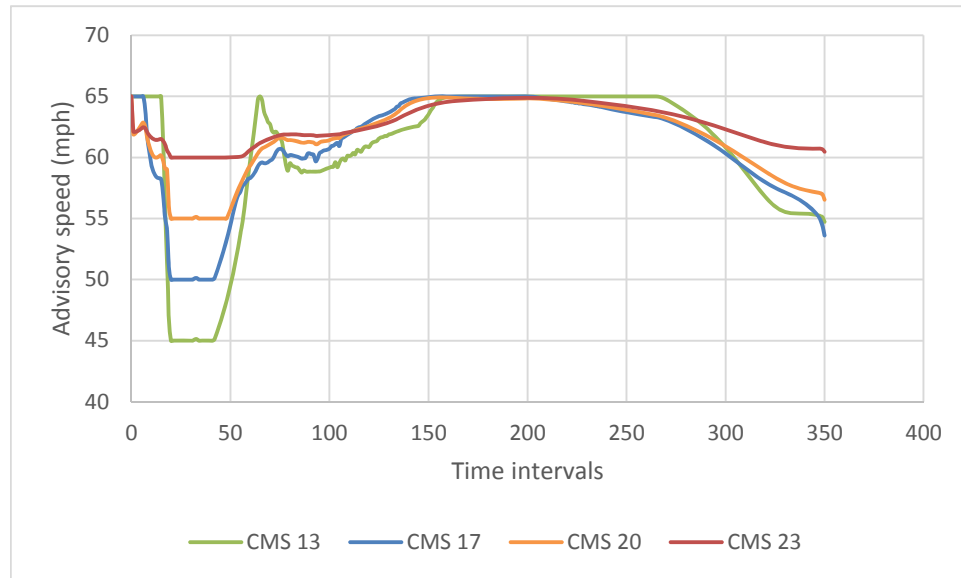
Figure 4-4: Optimal advisory speeds

To explore how the speed harmonization controls congestion propagation, Figures 4-5 and 4-6 display density (pc/mi/ln) variations for sections 7 to 11 in Base and when there is speed harmonization. These sections are located at upstream of work space and experienced density increase in the Base condition; however density in the section 11 did not exceed density at capacity (i.e. 45 pc/mi/ln) for 2-lane sections. Density in other sections exceed 35 pc/mi/ln which is the density at capacity for the work zone. Thus queue propagates roughly to 4 miles upstream of the work space and the maximum density for these sections are close to 50 pc/mi/ln.

When there is speed harmonization, arrival rate was controlled such that the density is around 35 pc/mi/ln (i.e. density at capacity for the work zone) or less for these sections. In particular when there is capacity drop, density drops to reduce arrival rate and congestion propagation rate; and after roughly interval 80 density for these sections is around density at capacity providing maximum exit flow rate.

The speed harmonization resulted in 20.4% ($=\frac{79.4-63.2}{79.4} * 100$) delay reduction. In particular, total delay for both Base and when there is speed harmonization are 79.4 veh-hr and 63.2 veh-hr, respectively and are computed as below:

$$Total\ delay = TTT - HVOL * N_t * \Delta t * TT_{SL} \qquad\qquad 4\text{-}14$$

Where TTT is the total travel time that is computed based on Equation 4.1; it is the objective function value multiplied by $L * \Delta t$. The second term in the Equation 4-14 is equal to total travel time under the speed limit. Each variable in the second term is defined as below:

$HVOL$:Hourly volume in vph,

N_t. Number of time intervals in the study period,

Δt: Interval length in hr, and

TT_{SL}: Travel time through the control sections under speed limit. Speed limit is 45 mph for the one-lane sections and it is 65 mph for the 2-lane sections.
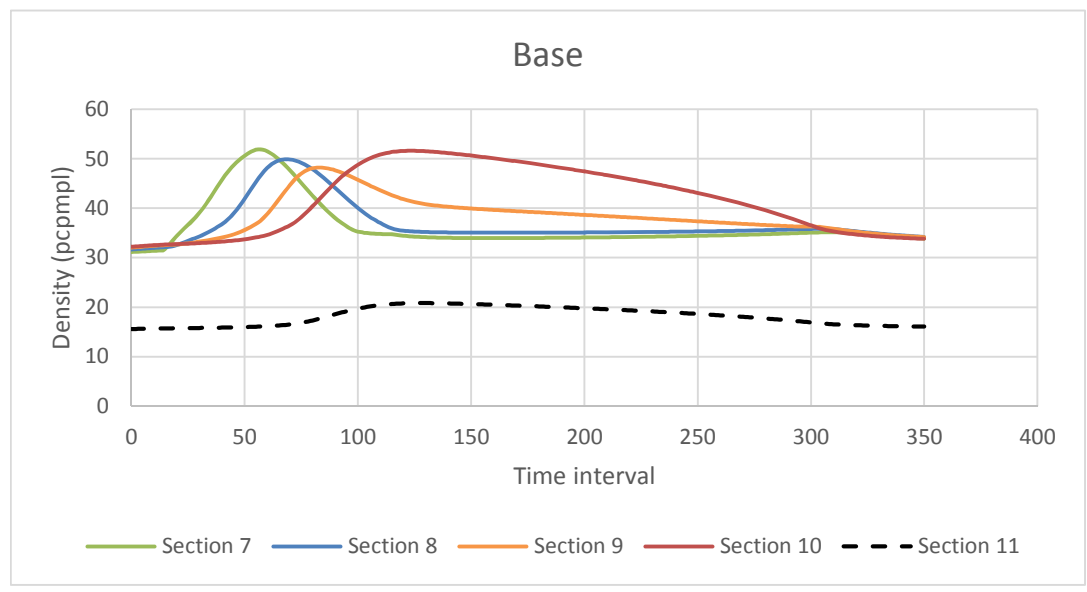
Figure 4-5: Density changes in Base conditions
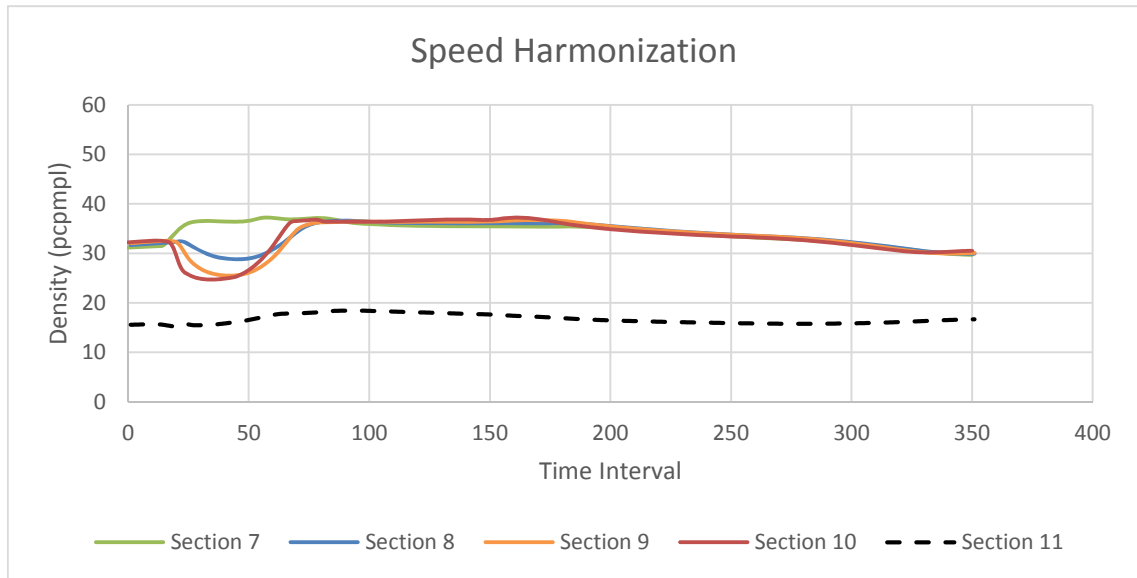
Figure 4-6: Density changes when there is speed harmonization

4.6 *Speed harmonization combined with rerouting*

In this section, speed harmonization is combined with rerouting strategy and the objective is to find the percentage of demand that should be rerouted from the mainline to achieve minimum travel time in the system (i.e. summation of travel time on the detour and the mainline).

The approach to find the diversion percentage assumes that the signs location is determined based on the base demand (i.e. when there is no diversion) and the locations are fixed when diversion occurs. For each diversion rate, optimal advisory speeds and corresponding travel time are determined. Also, total travel time on detour is computed under different diversion rate. The diversion rate that results in minimum total travel time in the system is determined.

Diversion rate is determined for a network shown in Figure 4-7. The mainline traffic conditions and work zone plan are the same as those for the benchmark problem in the Section 4-5. The length of the mainline is 20 miles with average travel time of 24.35 minute when there is no speed harmonization and no diversion. The time window to compute the average travel time is roughly 1.46 hr which is the same as analysis period to optimize speed harmonization.

The detour is represented by a 22-mile freeway link with 2 open lanes, free flow speed of 65 mph, and base volume of 1850 pcphpl. The speed-flow curve proposed by HCM 2010 for basic freeway sections with free flow speed of 65 mph is used to read traffic speed and compute travel time. Average travel time on the detour when there is no diversion is 21.24 minute.
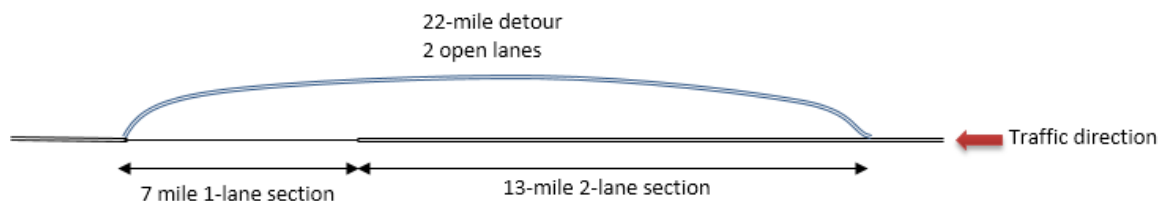
Figure 4-7: Mainline and detour sketch

Table 4-1 shows total travel time and total delay for different diversion volumes. For the
mainline, the optimized advisory speeds were found for the hourly volumes given in
Table 4-1 and total travel time was obtained from the objective functions. Delay was
computed based on the free flow speed of 65 mph for the 2-lane section and 45 mph for
the one-lane section. For the detour, average travel speed corresponding to each hourly
volume is read from the speed-flow curve and resulting average travel time for the 22-
mile detour is computed. Delay was computed based on the free flow speed of 65 mph.

Table 4-1: Travel time information on mainline and detour for different diversion rates

	Mainline with speed harmonization			Detour		
Diverted volume (pcphpl)	Hourly volume (pcphpl)	Total travel time (veh-hr)	Total delay (veh-hr)	Hourly volume (pcphpl)	Total travel time (veh-hr)	Total delay (veh-hr)
0	650	753.4	63.4	1850	1910.7	84.4
10	640	733.7	54.3	1860	1925.0	88.9
20	630	715.6	46.9	1870	1939.5	93.5
30	620	699.9	41.8	1880	1954.1	98.2
40	610	684.6	37.1	1890	1968.9	103.1
50	600	670.0	33.1	1900	1983.8	108.2
60	590	655.7	29.4	1910	1998.9	113.4

Figure 4-8 displays variation of total travel time in the system for different diversion
rates. The minimum travel time occurs when diversion rate is 40 pcphpl which is
corresponding to about 6% (=40/650) of the mainline traffic volume.
When there is no speed harmonization and no diversion total delay in the system is 163.8
veh-hr but when speed harmonization is combined with diversion total delay drops to
140.3 veh-hr which shows about 14.3% improvement in delay for the system.
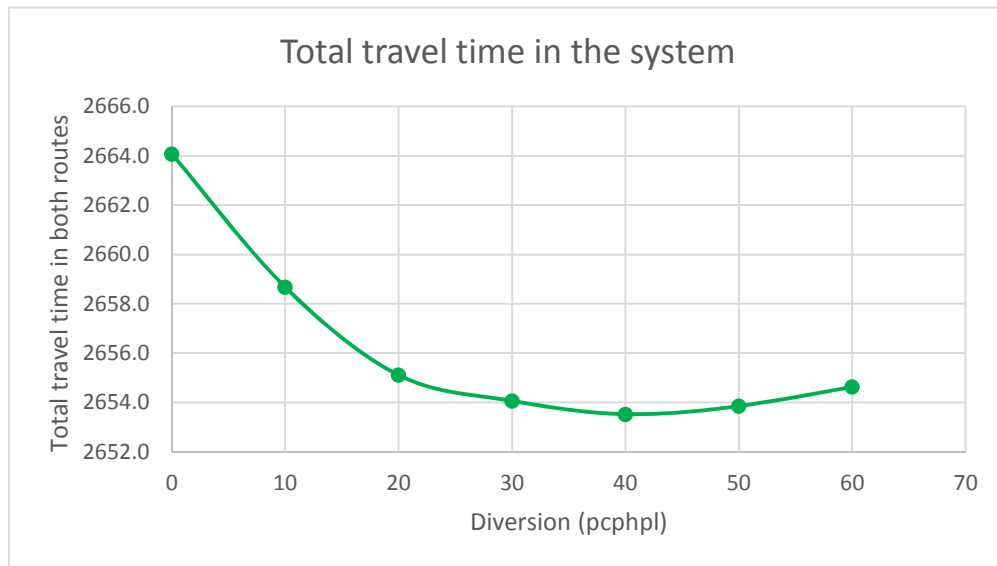
Figure 4-8: Total travel time in the system for different diversion rates

CHAPTER 5. EVALUATION OF SOLVERS FOR SPEED HARMONIZATION

Typically the programs that optimize speed harmonization (or variable speed limits) include many variables and constraints and for this reason past studies (Berton et al. 2004, Ghods et al. 2007) have applied Model Predictive Control (MPC) method to solve these problems. The potential drawback of this method is that the advisory speeds that are determined for a specific time interval are optimal for a time horizon which is shorter than the entire analysis period; however ideally it is preferred to optimize variables considering their effects over the entire analysis period.

In this study, one optimization program is solved for the entire analysis period; thus the program is a large scale optimization program. The objective of the section is to evaluate performance of some of the solvers to optimize speed harmonization. In particular, for different number of iterations, how the objective function values and feasibility error changes over the iterations are evaluated.

Six solvers that are available in NEOS website are selected for evaluation: CONOPT, IPOPT, Knitro, LOQO, Minos, SNOPT. The optimization program was written in AMPL and submitted to NEOS website for solution.

The benchmark problem is the same that in the Section 4.5. The optimization program roughly includes 71k variables and 86k constraints as reported by AMPL in the presolve stage.

To determine the signs location the algorithm was solved using IPOPT with 500 iterations. It turned out that the signs should be placed at sections 22, 18, 13, and 8.

Given the signs locations, the optimal advisory speeds were determined using each solver with four different iterations: 500, 700, 900, 1100. Also the solvers parameters were set up such that maximum feasibility error of 10^{-6} is achieved when solvers claim that the optimal solution is found. The other solvers parameters were set up to be default values.

The initial solution (i.e. the value of the variables at iteration zero) for all the variables in the program except advisory speeds are equal to those in the Base conditions. The performance of solvers are evaluated under two different initial solutions for the decision variable i.e. advisory speed:

INSOL1) Advisory speed is equal to traffic speed which is from the speed-flow curve: $AS_{i,t} = V_{i,t}$.

INSOL2) Advisory speed is equal to speed limit: $AS_{i,t} = MaxSL_i$

The results of evaluations are presented as below.

LOQO: How objective function and feasibility error change over the iterations are similar for INSOL1 and INSOL2. Figures 5-1a and 5-1b display the trend for INSOL1 and INSOL2, respectively when the maximum iteration is 1100. The primary axis (left) shows the objective function value and the secondary axis (right) displays the feasibility error. LOQO reports "suminf" which is sum of feasibility error and Figures 5-1a and 5-1b show that it stays very close to zero. The maximum suminf for INSOL1 and INSOL2 are 0.000072 and 0.000087, respectively. The objective function reaches to a stable solution roughly after iteration 260 for both initial solutions. The magnitude of objective functions for INSOL1 and INSOL2 are 181356.5 and 181246.9, respectively. The difference between the objective functions is equal to 0.45 veh-hr (see Equation 4-1); thus the objective function values are close.

43
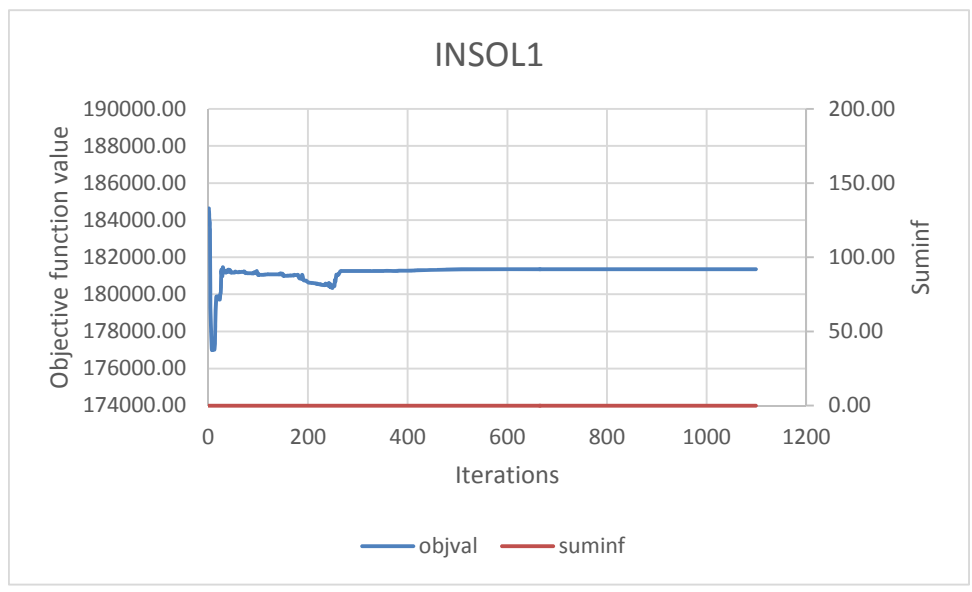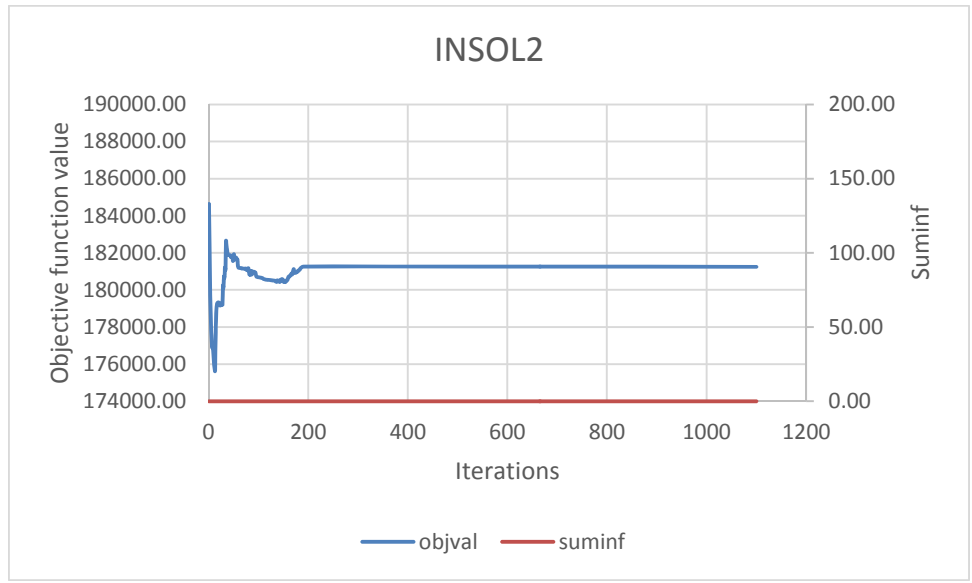
Figure 5-1 a

Figure 5-1 b

Figure 5-1: LOQO results for a) INSOL1 b) INSOL2

CONOPT: Overall CONOPT first tries to reduce sum of infeasibility and find a feasible solution. During this part the objective function value is zero. Then the solver starts improving the objective function for the feasible solution. For INSOL1 (see Figure 5-2a), it takes 440 iterations to find a feasible solution and then during the rest of iterations it improves the objective function.

For INSOL2 (see Figure 5-2b), there is no considerable infeasibility and the solver was improving the objective function from the fourth iteration. After 974 iterations, CONOPT stopped as the objective function was not practically improving.
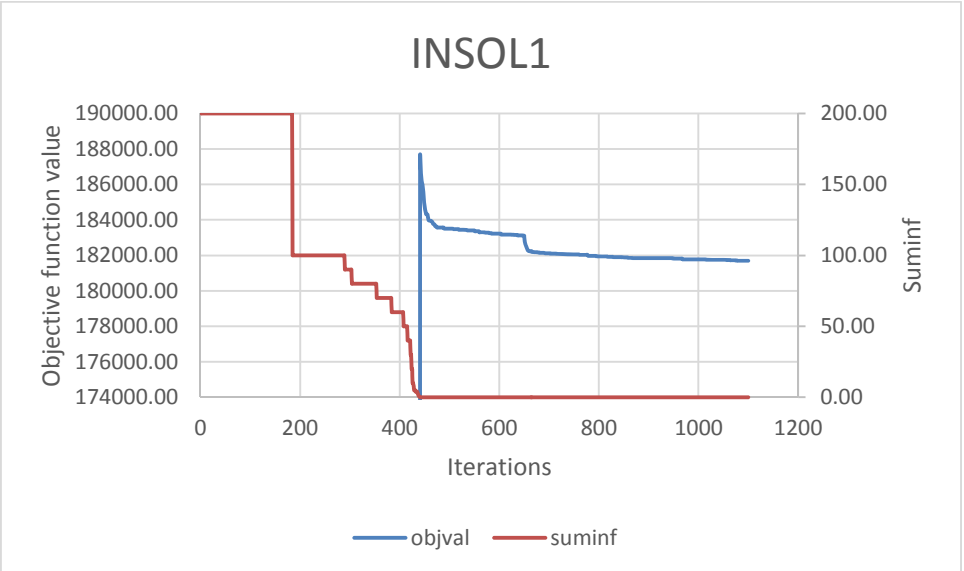
Figure 5-2 a
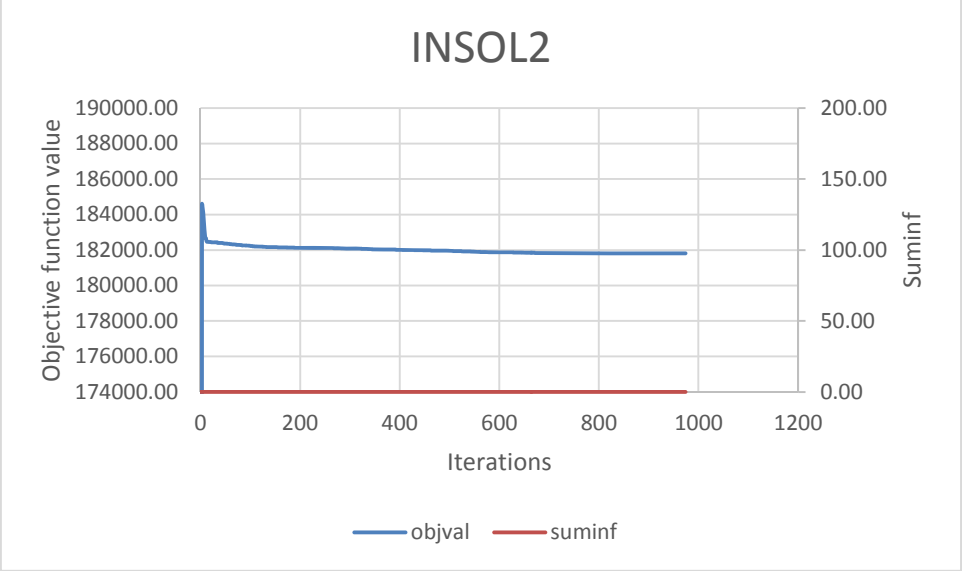
Figure 5-2 b

Figure 5-2: CONOPT results for a) INSOL1 b) INSOL2

IPTOP: As shown in Figure 5-3a for INSOL1, after 210 iterations the objective function reaches close to 180000, but the feasibility error values are above 2. (IPOPT reports the maximum absolute feasibility error rather than sum of them.). Thereafter, the solver searches if it is able to improve the objective function, however the amount of feasibility error is considerable (specially for the last iteration it is 11.90).

Similar trend exists for INSOL2 after 500 iterations; however feasibility error values are overall less than those for INSOL1; the feasibility error of the solution at iteration 1100 is 4.29.

KNITRO: As shown in Figure 5-4a, around iteration 575 the objective function value drops drastically while feasibility error is in the order of 1876. (KNITRO reports the maximum feasibility error.) Then the solver tries to reduce feasibility error over the rest of iterations. At the end the objective function value is 120193.9 with the feasibility error of 3.39. For INSOL 2 (See Figure 5-4b), KNITRO reaches to the objective function values of 181184.6 with feasibility error of 0.11 at iteration 755, but thereafter feasibility error or objective function increases. At iteration 1100 the solver returns an objective function value of 184948.3 with feasibility error of 0.24.
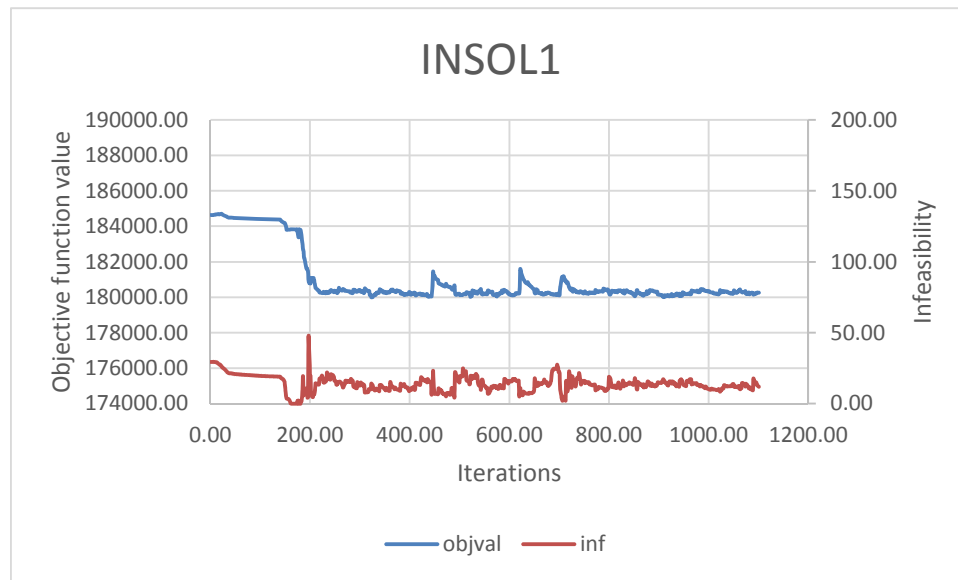
Figure 5-3 a
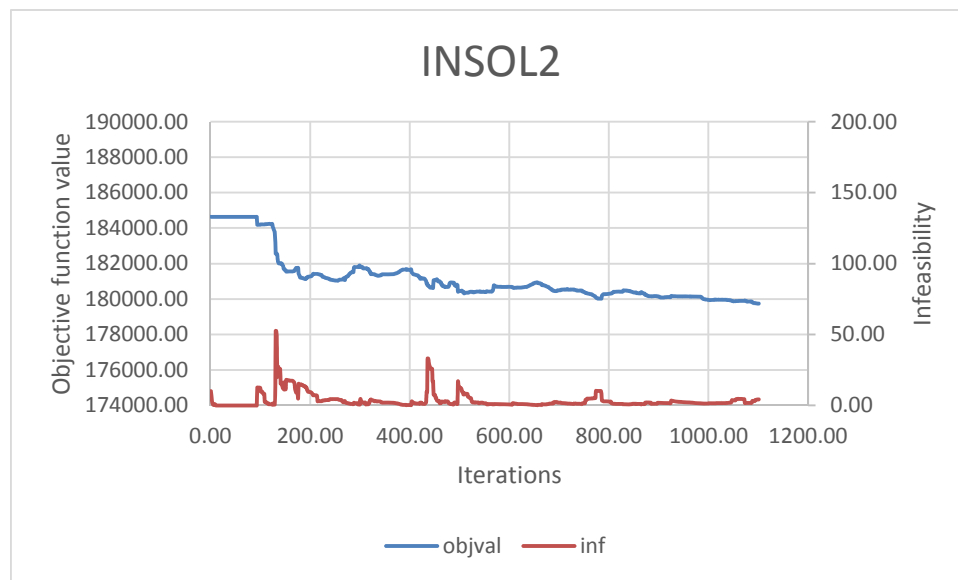
Figure 5-3 b

Figure 5-3: IPOPT results for a) INSOL1 b) INSOL2
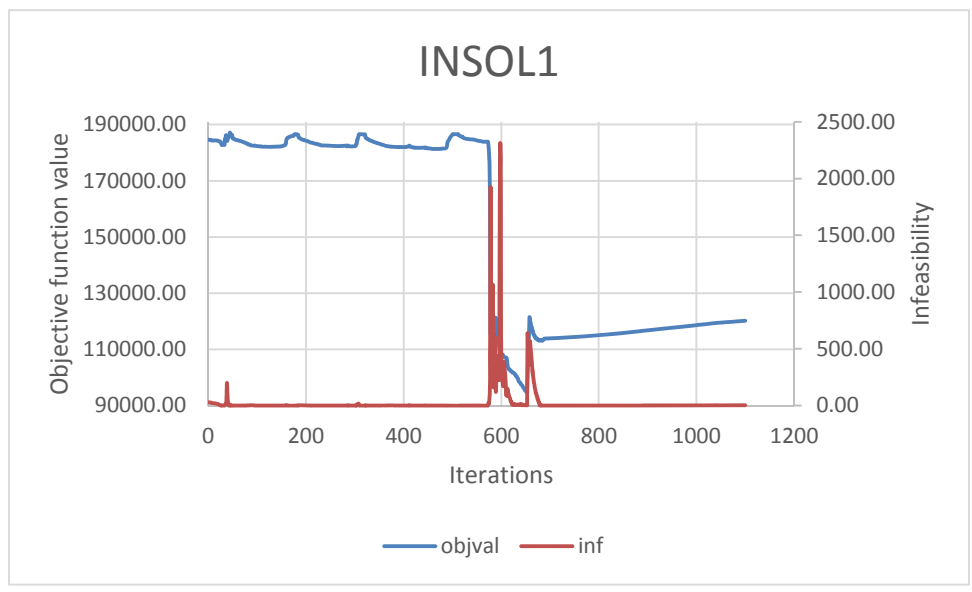
Figure 5-4 a
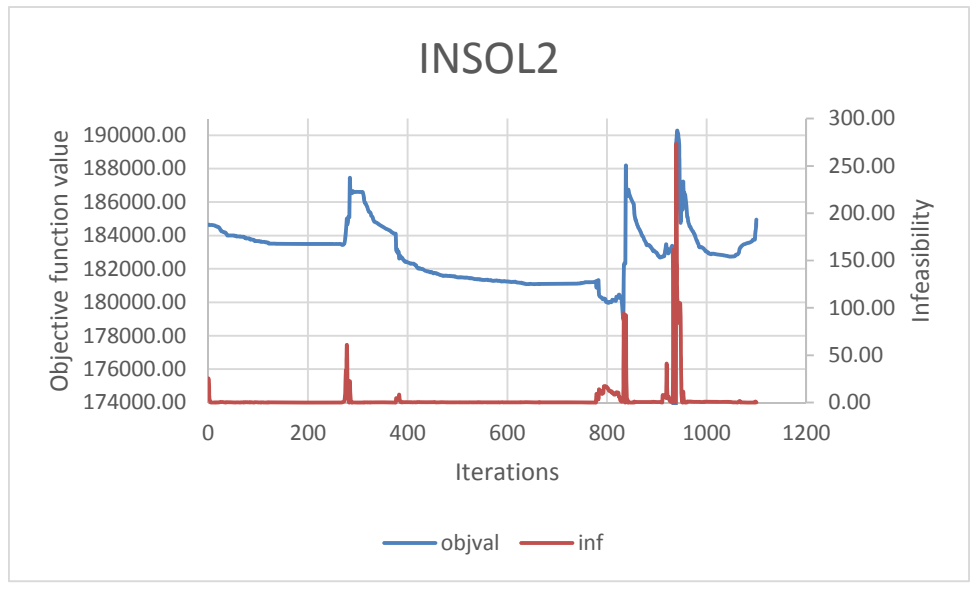
Figure 5-4 b

Figure 5-4: KNITRO results for a) INSOL1 b) INSOL2

MINOS and SNOPT: For both initial solutions the solver did not improve the initial solutions and they stopped.

5.1   Discussion of solvers

The performance of the solvers was evaluated under two different initial solutions for a minimization problem. The first initial solution was infeasible and the second one was feasible.

When the initial solution was infeasible, LOQO reached to a stable solution after 250 iterations. CONOPT spent about 440 iterations to find a feasible solution and over the rest of the iterations, it improved the solution but the objective function values was higher than that for LOQO. IPOPT and KNITRO did not reach to a stable solution but looking on the bright side, the solvers did not become trapped in local optimal solutions.

When the initial solution is feasible, both LOQO and CONOPT returned a feasible solution when the iteration limit reached; however the objective function value for LOQO was less (better) than that for CONOPT. IPOPT and KNITRO did not return a feasible solution at the end and the other solvers did not improve the initial solution.

This study intended to evaluate the solvers when all algorithm-related options (except feasibility error) are default values. For future study, it is recommended to investigate how the options should be set up for each solver to achieve the desirable performance.

The Minos and SNOPT developers claimed that the solvers will have the best performance when the number of variables and constraints are equal (or with few hundreds of degrees of freedom), but the difference between the number of constrains and variables was around 15000 in the benchmark problem. It is recommended to evaluate the performance of the solvers when the number of variables and constraints are close.

CHAPTER 6. CONCLUSIONS AND RECOMMENDATIONS

This study developed an optimization program and proposed a solution algorithm to find optimal advisory speeds and optimal Changeable Message Signs locations for work zones. . The proposed algorithm is iterative and the number of iterations is equal to the number of signs. At each iteration, the location that results in minimum travel time is determined. The algorithm was applied for a benchmark network where capacity drops for 10 minutes due to work intensity increase and traffic volume is close to the maximum capacity of the work zone. Results showed that speed harmonization can reduce delay by about 20%.

The study showed that single-regime fundamental relationships between traffic parameters may lead to an unexpected trend in congestion conditions; especially jam density might be too low (in the order of 100 pc/mi/ln). Thus, multi-regime models that were developed based on work zone field data were used in the optimization. The multi-regime models were approximated with simple functions to reduce complexity and avoid using if-then-else constraints or integer variables.

A preliminary evaluation of the six solvers for large scale optimization programs was conducted when default values were used for all algorithm-related options except options were set up to achieve feasibility error of 10^{-6} when solvers claim that optimal solution is found. The benchmark problem that included 71k variables and 86k constraints was solved for two different initial solutions. Results showed that solutions stay feasible over the iterations for LOQO and CONOPT while LOQO returns a slightly better (less) objective function value than CONOPT when iteration limit reached. The LOQO's objective function values were lower than CONOPT's by 0.19% and 0.31% for the two initial solutions.

It is recommended exploring how algorithm-related options should change to achieve desirable performance by each solver. The objective function in this study is to minimize total travel time in the control zone to improve traffic operation. It is recommended a multi-objective optimization program be developed to consider both safety and traffic operation measures in the objective function. Payne model was used as a constraint to determine speed dynamics in the roadway. It is recommended this model be compared with other second order models to determine advantages and disadvantages of each for work zones.

REFERENCES

Allaby, P.; Hellinga, B.; and Bullock, M., Variable speed limits: safety and operational impacts of a candidate control strategy for freeway applications. IEEE transaction 2007

American Highway Users Alliance, 1999-2004, Unclogging america's arteries: effective relief for highway bottlenecks, http://www.highways.org/pdfs/ bottleneck2004.pdf.

R. F. Benekohal, H. Ramezani, K. Avrenli, (2010) Delay and User's Cost in Highway Work Zones, Research Report FHWA-ICT-10-075. http://ict.illinois.edu/publications/report%20files/FHWA-ICT-10-075.pdf.

Breton, P.; Hegyi, A.; De Schutter,B.; Hellendoorn, H. , Shockwave elimination/reduction by optimal coordination of variable speed limit, IEEE proceeding 2002

Federal Highway Administration, ATDM program brief: an introduction to active transportation and demand management, http://www.ops.fhwa.dot.gov/publications/fhwahop12032/, 2012.

Federal Highway Administration, Manual on Uniform Traffic Control Devices, Sec. 6c.04, 2009

Ghods, A.; Rahimi Kian, A.; Tabibi, M.; A genetic-fuzzy control application to ramp metering and variable speed limit control, IEEE proceeding 2007

Ghods, A. ; Rahimi-Kian, A. A game theory approach to optimal coordinated ramp metering and variable speed limit. IEEE proceeding 2008

Hadiuzzaman, Md.; Qiu, T.; Cell transmission model based variable speed limit control for freeway. TRB 2012

Kamel, B.; Benasser, A.; Jolly D.; Flatness based control of traffic flow for coordination of ramp metering and variable speed limits. IEEE proceeding 2008

Kang, K.; Chang, G.; and Zou, N.; Optimal dynamic speed-limit control for highway work zone operations. TRR 2004

Kwon, E.; Brannan, D.; Shouman, K.; Isackson, C.; and Arseneau. B.; Development and field evaluation of variable advisory speed limit system for work zones. TRR 2007

Kwon, E.; Park, C.; Lau, D.; Kary, B.; Minnesota variable speed limit system: adaptive mitigation of shock waves for safety and efficiency of traffic flows. TRB 2012

Lin, P.; Kang, K,; Chang, G.; Exploring the effectiveness of variable speed limit controls on highway work-zone operations. Intelligent Transportation Systems, 8:1–14, 2004

Lu, X.; Qiu, t.; Varaiya P.; Horowitz, R.; Shladover, S.; Combining variable speed limits with ramp metering for freeway. Traffic Control American Control Conference, 2010

Lu, X.; Varaiya, P.; Horowitz, R.; Su, D.; Shladover, S.; A novel freeway traffic control with variable speed limit and coordinated ramp metering. TRB 2011.

McMurtry, T.; Saito, M.; Riffkin, M.; Heath, S.; Variable speed limits signs: effects on speed and speed variation in work zones. TRB 2008.

Papageorgiou, M.; Blosseville, J.; Hadj-Salem, H.; Macroscopic modeling of traffic flow on the boulevard Peripherique in Paris, Transportation Research Part B. pp. 29-47, 1989.

Park, B.; Yadlapati, S.; Development and testing of variable speed limit logics at work zones using simulation, TRB 2002.

Piao, J.; and McDonald, M.; Safety impacts of variable speed limits – a simulation study. IEEE proceeding 2008

Su, D.;Lu, X.;Varaiya, P.;Horowitz, R.;Shladover, S.; Variable speed limit and ramp metering design for congestion caused by weaving. TRB 2011

Wang, Y.; Ioannou, P.; A new model for variable speed limits. TRB 2011